J Korean Radiol Soc 2005;53:343 - 352

Differentiation Between Mass-forming Type Peripheral Cholangiocarcinoma and Hepatic Abscesses:
Application of Artificial Neural Networks to CT Images[1]

Nak Jong Seong, M.D., Jeong Min Lee, M.D., Se Hyung Kim, M.D., Joon Koo Han, M.D., Young Jun Kim, M.D., Ji Hoon Kim, M.D., Jae Young Lee, M.D., Seong Ho Park, M.D.[2], Byung Ihn Choi, M.D.

Purpose: To determine which CT findings are useful for differentiating cholangiocarcinomas (CC) from hepatic abscesses and also to determine whether artificial neural networks (ANNs) improve radiologists' performance.

Materials and Methods: CT findings of 51 patients with mass-forming type CC and 70 patients with hepatic abscesses were analyzed with morphologic, enhancing and other ancillary findings by three radiologists with differing levels of expertise independently. ANNs were constructed using statistically significant CT findings derived from the analyses. The performances of the ANNs and the radiologists were evaluated using receiver operating characteristic analysis.

Results: CT findings of rim-like enhancement, lymphadenopathy, capsular retraction, focal bile duct dilatation and a solid component were significant features of CC ($p < 0.05$). Findings of a clustered sign, multilayered enhancement, sharp margin, round shape, and air-biliary gram were significant features of hepatic abscesses. The ANNs showed better performance (AZ = 0.9673, 98.0%, 97.1%, and 97.5%, respectively) than the resident (AZ = 0.898, 78.4%, 81.4%, 80.2%) ($p < 0.05$) in differentiating between the two diseases: (AZ, sensitivities, specificities, and overall accuracies). However, there were no significant differences in the diagnostic performance of the ANNs and the two board-certified radiologists.

Conclusion: Several CT findings are useful in differentiating CC from hepatic abscesses and ANNs may improve the performance of a radiologist with little experience.

Index words : Abdomen, CT
Bile duct, neoplasm
Liver, abscess
Computers, neural network
Diagnostic radiography, observer performance

Several CT features of hepatic abscesses have been reported (1 - 4). Some hepatic abscesses occasionally mimic other hepatic tumors on CT, and some malignant hepatic tumors such as metastases, cholangiocarcinoma (CC), and leiomyosarcoma, may also mimic hepatic abscesses (5 - 12). Since the treatment strategy differs based on the possibility of malignancy, differentiation of hypovascular liver tumors such as CC or metastasis from hepatic abscesses on CT is important. A variety of radiologic procedures have been used to evaluate focal

[1]Department of Radiology and the Institute of Radiation Medicine, Seoul National University Hospital and [2]Asan Medical Center
Received April 25, 2005 ; Accepted August 4, 2005
Address reprint requests to : Jeong Min Lee, M.D., Department of Radiology, Seoul National University College of Medicine
28, Yongon-dong, Chongno-gu, Seoul 110-744, Korea.
Tel. 82-2-2072-3154 Fax. 82-2-743-6385 E-mail: leejm@radcom.snu.ac.kr

liver lesions, with CT currently considered one of the most important noninvasive diagnostic techniques for characterizing focal liver lesions (7, 8). Although CT findings of these two diseases have been published in several articles (1 - 4, 13 - 15), differentiating CC from hepatic abscesses, even using sonography, enhanced CT or MRI, remains a difficult task for radiologists because there is an overlapping spectrum of radiographic appearances and clinical parameters between the two diseases (10, 11, 16, 17). However, to our knowledge, there are no reports investigating the usefulness of helical CT for differentiating CC from hepatic abscesses in a large patient population.

In recent years artificial neural networks (ANNs) have been studied intensively computer scientists and have been shown to be a powerful tool for a variety of data-classification and pattern-recognition tasks. However, the usefulness of ANNs in diagnostic radiology has focused mainly on chest and breast lesions and in the diagnosis of pulmonary nodules, interstitial lung disease, pediatric lung lesions, and breast nodules (18 - 23).

The purpose of this study is to determine which CT findings are useful for differentiating CC from hepatic abscesses and to compare the performance of ANNs applied to CT images with the performance of radiologists with differing levels of expertise in differentiating between the two diseases using receiver operating characteristic (ROC) analysis.

Materials and Methods

Patient Population

In order to find patients diagnosed with hepatic abscesses and mass-forming type CC, a computerized search of the electronic medical records including radiologic, surgical, and pathologic reports from January 1998 to March 2003 at the Seoul National University Hospital, was performed. Due to the retrospective nature of the study and because the institution's patients sign a general consent form to cover all diagnostic studies, neither institutional review board approval nor informed consent was necessary.

The computerized search of the electronic medical records revealed 380 patients diagnosed with hepatic abscesses. Two abdominal radiologists, who did not participate in the image interpretation, reviewed the available CT scans for these patients and selected patients for subsequent analysis. Of these patients, 310 were excluded from analysis for the following reasons: (a) no contrast-enhanced helical CT scan was available ($n = 75$); (b) the presence of associated malignancy ($n = 125$) such as hepatocellular carcinoma ($n = 32$), gastric cancer ($n = 20$), previous klatskin tumor ($n = 17$), colorectal cancer ($n = 13$), pancreatic cancer ($n = 10$), other malignancies ($n = 17$), and unknown origins ($n = 16$); and (c) no histologic confirmation of hepatic abscesses or insufficient imaging follow-up ($n = 110$). The remaining 70 patients (48 male, 22 female; mean age 58.2 years; range 29-91 years) with hepatic abscesses were included in this study. Pyogenic abscesses were confirmed by positive cultures from percutaneous aspirates in 31 patients. Five of these 31 patients had monomicrobial abscesses and 26 patients had polymicrobial abscesses. In the remaining 39 patients that showed no growth of the abscess contents, a diagnosis of hepatic abscess was based on symptoms including fever and abdominal pain, laboratory results such as leukocytosis, and the CT imaging findings. All of these 39 patients responded to percutaneous drainage and/or antimicrobial therapy, and subsequent CT scanning revealed improvement of their hepatic abscesses.

The computerized search of the electronic medical records revealed 175 patients diagnosed with intrahepatic CC. Of these patients, 124 were excluded from analysis for the following reasons: (a) no contrast-enhanced helical CT scan was available ($n = 107$); (b) other types of CC were present ($n = 12$; periductal infiltration in nine patients and intraductal-growing in three); and (c) hyperattenuating mass ($n = 5$) on CT scans. The remaining 51 patients (37 male, 14 female; mean age 55.4 years; range 40 - 80 years) with the mass-forming type CC were included in the study. CC was confirmed by percutaneous ultrasound-guided needle biopsy in 40 cases and by surgery in 11 patients.

CT Acquisition

The CT examinations were performed on four different scanners (Somatom Plus S and Somatom Plus 4; Siemens Medical Systems, Erlangen, Germany; HiSpeed Advantage CT scanner; General Electric Medical Systems, Milwaukee, WI; MX 8000; and Marconi Medical Systems, Highland Heights, OH). Due to the retrospective nature of the study several different CT techniques were used. In general, examinations were performed using a spiral technique with 5 - 10 mm collimation and 5 - 10 mm reconstruction intervals. The X-ray tube voltage was 120 - 140 kV, and the current varied between 150 and 200 mA. During this period

(January 1998 to March 2003), the standard protocol for dynamic CT consisted of a total volume of 120 - 150 mL of nonionic intravenous contrast material (300 - 370 mg of iodine per mL) administered by power injection at a rate of 2 - 3 mL/sec, with a scanning delay of 30 seconds for the hepatic arterial phase (HAP) and of 65 seconds for the portal venous phase (PVP). Of the 121 patients analyzed, 101 (56 with hepatic abscesses and 45 with CC) underwent dual-phase (HAP and PVP) CT and the remaining 20 (14 with hepatic abscesses and six with CC) underwent single-phase (PVP) CT.

Radiologists CT Interpretation

Each of the 121 CT image sets were analyzed retrospectively and independently by three radiologists (one faculty-level abdominal radiologist with 20 years experience, one abdominal imaging fellow with 8 years experience, and one senior resident with 3 years experience) who were unaware of the final diagnosis and of any clinical or laboratory findings. When a patient had multiple lesions, only the largest lesion was analyzed.

Based on previous reports on hepatic abscesses and CC (1 - 4, 7, 8, 13 - 15), several imaging features suggestive of hepatic abscesses and CC were chosen by the study coordinators. The three radiologists were given a short summary of what had been reported as "typical findings" of hepatic abscesses and CC, including morphologic features and enhancing characteristics of the lesions and other findings such as lymphadenopathy and metastases (Table 1). The three radiologists independently reviewed all 121 CT scans at a picture archiving and communications system (PACS) workstation (Marotech, Seoul, Korea) without knowledge of the tissue diagnosis or clinical course. During the analysis of the CT images, cases of CC and hepatic abscesses were presented randomly. The readers were asked to grade their degree of confidence for the presence of various CT findings believed to be indicative of the two diseases and for each diagnosis. During the review, the radiologists were allowed to adjust the window width and length to interpret the CT images. In the CT interpretation, the portal venous phase (PVP) was used as the core image set because the lesions are seen the best during PVP. The degree of confidence for each diagnosis was graded as follows: 1, definitely benign (abscess); 2, probably benign; 3, possibly malignant; 4, probably malignant; and 5, definitely malignant. The degree of confidence for the presence of each of the CT findings indicating hepatic abscesses or CC was graded as follows: 1, definitely absent; 2, probably absent; 3, possibly present; 4, probably present; and 5, definitely present.

Table 1. Useful CT Findings in Differentiating Peripheral Cholangiocarcinoma from Hepatic Abscesses

Cholangiocarcinoma	Hepatic Abscess
Broad marginal transition	Sharp marginal transition
Spiculated outer margin	Round outer margin
Solid component	Cystic component
Rim-like enhancement	Multilayered enhancement
Lymph node enlargement	Internal air density
Capsular retraction	Clustered sign
Focal bile duct dilatation	Air-biliary gram
	Transient hepatic attenuation difference

CT findings were derived from references 1 - 4 and 13 - 15.

The CT findings were analyzed according to two categories; the lesion itself and the associated findings. The lesion was evaluated for margin (sharp vs ill-defined), configuration (unilocular vs clustered), shape (lobulated vs round), the presence of a solid component and internal air-density, and the pattern of enhancement (rim-like vs multilayered). Associated findings included stones in the IHD or CBD, the presence of capsular retraction, lymphadenopathy (short-axis diameter of lymph nodes more than 1 cm or the presence of central necrosis), focal biliary dilatation distal to the lesion, air-biliary gram, transient hepatic attenuation difference (THAD), ascites, pleural effusion, atelectasis of the lower lung, and extrahepatic metastasis.

Extraction of Significant Imaging Features

A biostatistician participated in the study design and review of the data. Statistical differences of the CT findings between abscesses and CC were analyzed using Fisher's exact test and the Chi-square test. The odds ratio (OR) for each CT feature used to characterize the lesion into an abscess or CC, was also obtained. The magnitude of the relevance of statistically significant CT predictors of abscesses or CC was ranked according to their P values and ORs. We used binary collapse of the rated responses for statistical analysis. Specifically, lesions that were graded with scores of 1 and 2 were classified as an abscess, and scores of 3, 4, and 5 were classified as CC. Each CT finding that was graded with a score of 1 or 2, was classified as absent, whereas, scores of 3, 4, and 5 were as classified as having that CT finding.

Artificial Neural Networks

A brief search of possible ANN designs provided in-

sight into the type of design that would work for this application. Several designs were attempted and rated for their ability to generalize, once trained. In the present study, fully connected, three-layer ANNs with a back propagation algorithm were used. The ANNs consisted of one input layer, one hidden layer and one output layer. Statistically significant CT features derived from the Chi-square or Fisher's exact test were used as input variables for the input layer. The hidden layer consisted of 15 neurons connected to the input layer. A nonlinear, sigmoid function was used as a transfer function for each of the neurons in the hidden layer and the output layer of the networks. The nonlinear function is expressed by: $f(\sum_i x_i w_i) = \frac{1}{1+e^{-\sum x_i w_i}}$, where $f(\sum_i x_i w_i)$ is the output of a neuron i and xiwi is the net input to the neuron, which was derived by multiplying the weight (w) by the input value (x) of the unit. During the training process, the connection weights between the neurons were adjusted using the back propagation updating algorithm (23). The hidden layer was connected to the output layer of a single neuron which indicated whether the CT findings were classified as benign (abscess) or malignant (CC).

The training and testing of the ANNs were performed by means of a leave-one-out method. With this method, all of the cases in the database except for one were used for training; the case that was not used was used in the testing of the trained ANNs. We used a fourfold cross-validation procedure for the training procedure. Each of the four different networks was trained until the error in the training set reached the stopping criterion. This procedure was repeated until every case in the database was used once for testing. The test results of the four different networks were combined to calculate ANNs' performance in terms of determining the malignancy of the lesion. The output values for the test were between 0 and 1, which is used to represent the likelihood of malignancy. A threshold value of 0.5 was used, above which all values were regarded to be malignant.

ROC Analysis

The individual performances of the three radiologists and of the ANNs were evaluated by ROC analysis; areas were calculated using a nonparametric method (24, 25). Binormal ROC curves were estimated using the MedCalc software, version 7.1 (MedCalc Software, Mariakerke, Belgium) which was used to obtain maximum-likelihood estimates of binormal ROC curves from the continuous ordinal-scale rating data. The AZ was calculated to summarize the performance of each radiologist and the ANNs in the task of classifying hepatic abscesses and CC. The univariate z-score test was used to assess the significance of differences in the area (AZ) under the two estimated binormal ROC curves. In addition, sensitivity and specificity were calculated using only those patients deemed to have CC by each radiologist and those with ANNs output levels of 0.5 or greater. Sensitivity and specificity were presented with 95% confidence intervals (CI).

Statistical Analysis

Statistical differences of the CT findings between abscesses and CC were analyzed using Fisher's exact test and the Chi-square test. Interobserver agreements among the three radiologists for each CT finding and the final radiologic diagnosis were evaluated using the Cronbach coefficient α where an αvalue of greater than 0.8 was considered to represent excellent agreement and αvalues of 0.70 - 0.80 represented good agreement. Values of less than 0.70 were considered to represent poor agreement (25, 26). Statistical analyses were performed using SPSS software, version 11.0 for Windows (SPSS Inc., Chicago, Ill). A probability value of less than 0.05 was considered to indicate statistical significance. To compare the performance of each radiologist and the ANNs, the sensitivity and specificity of the ANNs and each reviewer were compared using the McNemar test, which is a nonparametric test for two related dichotomous variables.

Results

Interobserver agreements among the three radiologists in recognizing the CT findings are presented in Table 2. With respect to the presence of air density within the lesion, the three radiologists were in complete agreement ($\alpha = 1.00$). In terms of most of the CT features analyzed, almost perfect (for clustered appearance and multilayered enhancement of the lesion, capsular retraction, focal biliary dilatation distal to the lesion, air-biliary gram, lymphadenopathy, THAD, atelectasis of the lower lungs, and pleural effusion) or substantial agreement (rim-like enhancement of the lesion, solid component within the lesion, sharp margin, and configuration of the lesion) was achieved. For specific diagnosis, interobserver agreement among the three radiologists was almost perfect ($\alpha = 0.907$). In addition, interobserver agreement of each combination of two radiolo-

gists was also almost perfect (αbetween faculty radiologist and fellow; 0.923, αbetween faculty and resident; 0.828, αbetween fellow and resident; 0.838).

Significant CT features for hepatic abscesses and CC are listed in descending order of OR and 95% confidence interval (CI) in Tables 3 and 4, respectively. The presence of air density with the lesion, of which OR could not be calculated, was significantly associated with hepatic abscesses ($p=0.002$). In addition, hepatic abscesses were significantly associated with the presence of the following CT features: clustered appearance of the lesion; a sharp margin; multilayered enhancement; air-biliary gram; configuration; atelectasis; pleural effusion; and THAD (Figs. 1 & 2). The largest OR was observed in the cluster sign (OR=55.56) which indicates that the predicted risk associated with the presence of

Table 2. Interobserver Agreement of CT Findings and Diagnosis among Three Readers

CT Findings and Diagnosis		αValues
CT Findings	Internal air density	1.00 (perfect)
	Air-biliary gram	0.97 (excellent)
	Ascites	0.91 (excellent)
	Atelectasis of lower lung	0.91 (excellent)
	Multilayered enhancement	0.90 (excellent)
	Diffuse bile duct dilatation	0.90 (excellent)
	Pleural effusion	0.89 (excellent)
	Capsular retraction	0.88 (excellent)
	Cluster sign	0.87 (excellent)
	Biliary stone	0.86 (excellent)
	Focal bile duct dilatation	0.85 (excellent)
	Transient hepatic attenuation difference	0.84 (excellent)
	Lymph node enlargement	0.82 (excellent)
	Presence of solid component	0.80 (good)
	Peripheral rim-like enhancement	0.76 (good)
	Margin of the lesion	0.75 (good)
	Configuration of the lesion	0.72 (good)
	Vascular thrombosis	0.69 (poor)
Diagnosis	Among three readers	0.91 (excellent)
	Between faculty and fellow	0.92 (excellent)
	Between faculty and resident	0.83 (excellent)
	Between fellow and resident	0.84 (excellent)

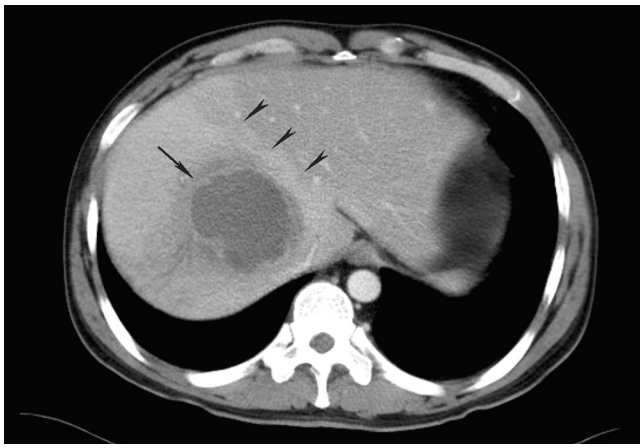

Fig. 1. 41-year-old man with a hepatic abscess.
Axial contrast-enhanced CT scan shows a hypoattenuating mass with a multi-layered enhancing wall (black arrows) in the right lobe of the liver. Note diffuse hepatic parenchymal enhancement with a straight border (arrow heads).

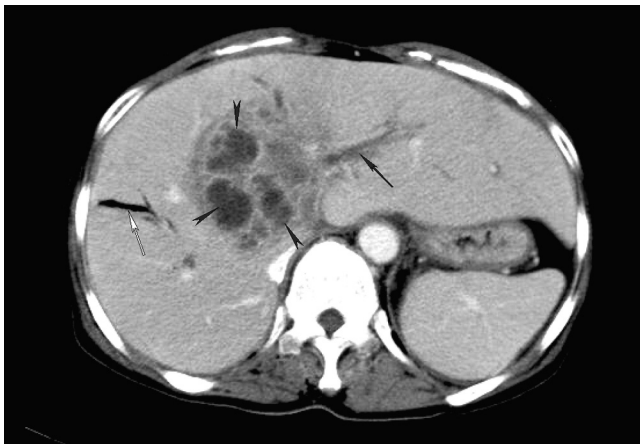

Fig. 2. 59-year-old woman with a hepatic abscess with cluster sign.
Axial contrast-enhanced CT scan shows a multi-septated hypoattenuating lesion with cluster sign (arrow heads) and multilayered wall enhancement. Note the intrahepatic ductal dilatation (black arrow) and the air biliary gram in segment 5 (white arrow).

the cluster sign on CT was 55.56 times higher for patients with hepatic abscesses than those with CC.

The CT features of peripheral rim-like enhancement, lymphadenopathy, capsular retraction, focal biliary dilatation distal to the lesion, and a solid component within the lesion were significant for diagnosing CC (Figs. 3 & 4). The largest OR was observed in the rim-like enhancement of the lesion (OR = 49.78) (Fig. 3).

Tables 5 and 6 list the diagnostic performances of radiologists and the ANNs in terms of AZ, sensitivity and specificity in diagnosing CC. The performance of the ANNs (0.966, 95% CI: 0.916, 0.990), the faculty level radiologist (0.947, 95% CI: 0.891, 0.979), and the radiologic fellow (0.946, 95% CI: 0.889, 0.978) were significantly better in terms of AZ than that of the resident (0.873, 95% CI: 0.800, 0.926) based on the outcome of the z-score test ($p < 0.049$). However, the performance between the ANNs, faculty, and fellow were not significantly different ($p > 0.05$). For diagnosing CC at a rating of 3 or larger, the sensitivities of the faculty (48/51, 94.1%; 95% CI: 0.835, 0.986), fellow (48/51, 94.1%; 95% CI: 0.835, 0.986), and the ANNs (49/51, 96.1%; 95% CI: 0.865, 0.995) were significantly better than that of the resident (40/51, 78.4%; 95% CI: 0.652, 0.877) ($p < 0.05$). However, the differences in sensitivity between the two radiologists (faculty and fellow) and the ANNs were not statistically significant according to the results of the McNemar test ($p > 0.05$). For diagnosing an abscess at a rating of 1 or 2, the sensitivity was the same as the specificity for diagnosing the CC of ANNs (68/70, 97.1%; 95% CI: 0.901, 0.997) and was statistically better than that of the resident (57/70, 81.4%; 95% CI: 0.706, 0.890) ($p = 0.005$) (Table 6). However, the specificities from the

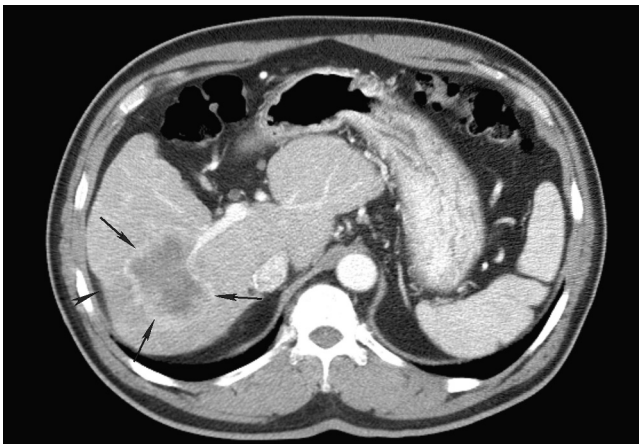

Fig. 3. 57-year-old man with cholangiocarcinoma.
Axial contrast-enhanced CT scan shows an irregular mass with rim-like enhancement (black arrows) and capsular retraction (arrow head).

Table 3. Significant CT Findings for Cholangiocarcinoma and their Odds Ratio

CT Findings	Odds Ratio	Odds Ratio		*p* value
		95% Confidence Interval		
		Lower	Upper	
Peripheral rim-like enhancement	49.78	16.51	150.12	< 0.0001
Lymph node enlargement	21.94	4.83	99.73	< 0.0001
Capsular retraction	21.23	2.66	169.51	< 0.0001
Focal bile duct dilatation	16.94	4.70	61.09	< 0.0001
Presence of solid component	8.41	3.18	22.24	< 0.0001

Table 4. Significant CT Findings for Hepatic Abscesses and their Odds Ratio

CT Findings	Odds Ratio	Odds Ratio		*p* value
		95% Confidence Interval		
		Lower	Upper	
Inner air density	Specific finding	-	-	0.002
Cluster sign	55.56	7.35	500.00	< 0.0001
Multilayered enhancement	29.41	6.54	125	< 0.0001
Sharp margin	21.28	8.00	55.56	< 0.0001
Air-biliary gram	12.50	1.59	100	0.004
Configuration	10.64	4.18	27.03	< 0.0001
Atelectasis of lower lungs	9.43	3.72	23.81	< 0.0001
Pleural effusion	6.90	2.44	19.61	< 0.0001
THAD	2.75	1.30	5.81	0.01

THAD = transient hepatic attenuation difference.

three radiologists were not significantly different from each other (faculty; 63/70, 90.0%, 95% CI: 0.905, 0.954, fellow; 61/70, 87.1%, 95% CI: 0.771, 0.933, resident; 57/70, 81.4%, 95% CI: 0.706, 0.890) ($p > 0.05$).

Discussion

Differentiating between hepatic abscesses and mass-forming type intrahepatic CC on CT remains a difficult problem because a considerable overlap between their

Table 5. Diagnostic Performances of Three Radiologists and ANNs for Diagnosing Cholangiocarcinoma using Receiver Operating Characteristic Analysis

	AZ					
	Value	95% CI		*p* value†		
		Upper	Lower	For ANNs	For Faculty	For Fellow
Faculty	0.947	0.891	0.979	0.359	-	0.957
Fellow	0.946	0.889	0.978	0.448	0.957	-
Resident	0.873	0.800	0.926	0.012	0.049	0.041
ANNs	0.966	0.916	0.990	-	0.359	0.448

†Two-tailed *p* values were calculated between each reader and the ANNs from the univariate z-score test. ANNs = artificial neural networks, CI = confidence interval

Table 6. Sensitivities and Specificities of Three Radiologists and ANNs for Diagnosing Cholangiocarcinoma

	Sensitivity						Specificity					
	Value	95% CI		*p* value†			Value	95% CI		*p* value†		
		Upper	Lower	For ANNs	For Faculty	For Fellow		Upper	Lower	For ANNs	For Faculty	For Fellow
Faculty	94.1 (48/51)	0.835	0.986	1.000	-	1.000	90.0 (63/70)	0.805	0.954	0.165	-	0.791
Fellow	94.1 (48/51)	0.835	0.986	1.000	1.000	-	87.1 (61/70)	0.771	0.933	0.055	0.791	-
Resident	78.4 (40/51)	0.652	0.877	0.015	0.041	0.041	81.4 (57/70)	0.706	0.890	0.005	0.227	0.487
ANNs	96.1 (49/51)	0.865	0.995	-	1.000	1.000	97.1 (68/70)	0.901	0.997	-	0.165	0.055

* Data in parentheses are the numbers from which the proportions were calculated. † *p* values were calculated between each reader and the ANNs from the McNemar chi-square test. ANNs = artificial neural networks, CI = confidence interval.

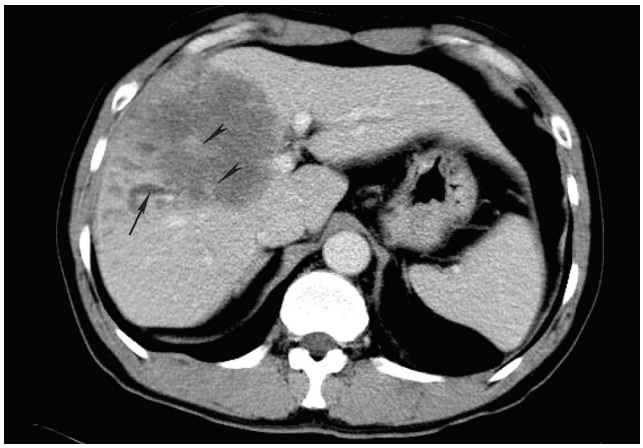

Fig. 4. 55-year-old man with cholangiocarcinoma presenting with fever and vague right upper quadrant pain.
Axial contrast-enhanced CT scan shows a large hypoattenuating mass with focal bile duct dilatation (black arrow). The presence of a heterogeneously enhancing solid component of the mass (arrowheads) and the absence of a multi-layered enhancing pattern or transient hepatic attenuation difference helps to determine the diagnosis of cholangiocarcinoma.

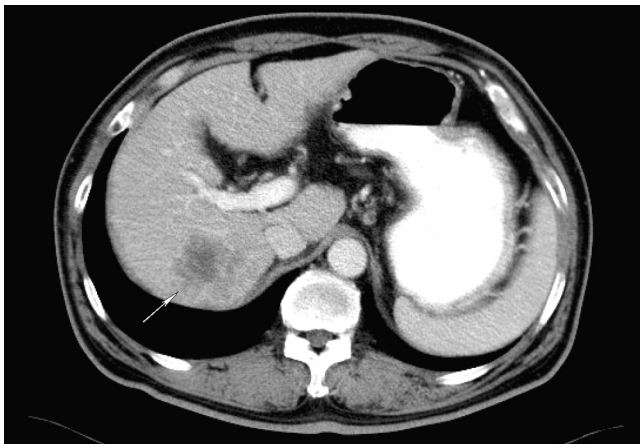

Fig. 5. 56-year-old man with cholangiocarcinoma and accompanying fever and leukocytosis.
Axial contrast-enhanced CT scan shows a low attenuating lesion with multi-layered enhancement (arrow) in the right posterior segment of the liver, which mimics a hepatic abscess. The resident reviewer diagnosed this lesion as a hepatic abscess, but the other radiologists correctly diagnosed it as cholangiocarcinoma.

clinical presentations and radiologic appearance may exist (9 - 11, 17, 27). Despite that, there have been many reports on CT findings of hepatic abscesses (1 - 4) and CC (13 - 15), with CC often being misinterpreted as a hepatic abscess and mistreated with percutaneous drainage which can cause tract seeding or peritoneal spillage of the tumor (28). Many previous studies have described simple observations of the CT findings for each disease, but no study has attempted to provide differential points by dedicated statistical analysis or to develop diagnostic algorithms to differentiate them. Recently, several publications have focused on the application of ANNs for lesion classification in the field of radiology (29 - 31). In this study, we attempted to construct ANNs to differentiate hepatic abscesses from CC on CT and to determine whether ANNs are able to improve radiologists' performance in differentiating between the two diseases.

The ANNs constructed for this study using significant CT findings derived from univariate analysis as multiple input variables showed a high performance in differentiating between hepatic abscesses and CC. The AZ value, sensitivity and specificity of the ANNs were significantly greater than those of the resident and marginally better than those of the other radiologists. However, there were no statistically significant differences between the ANNs and the two radiologists. Considering the excellent agreement for each CT finding among the three radiologists, the low performance of the resident is perhaps explained by the fact that a resident may not be able to effectively organize all of the CT features systematically. On the other hand, ANNs consistently and comprehensively respond to all data that has been input. In addition, it was expected that the experienced radiologists were aware of the relative importance of the significant CT findings based on their experience in dealing with various CT findings, which was used to help differentiate between the two diseases. Therefore, we are not surprised at the excellent performance shown by the ANNs and the abdominal radiologists in differentiating between the two diseases. We believe that the inclusion of a fellow and a resident as reviewers makes our results and conclusions more applicable for individuals with varying levels of experience.

In this study, hepatic abscesses were characterized by lesions having inner air-density, cluster sign, multilayered enhancement, sharp margin, and a lobulated configuration. In addition, hepatic abscesses were also more frequently associated with air-biliary gram, atelectasis of the lower lungs, pleural effusion, and transient hepatic attenuation difference (THAD). On the other hand, lesions showing peripheral rim-like enhancement, capsular retraction, focal bile duct dilatation distal to the lesion, a solid component or which had lymph node enlargement, were more frequently associated with patients with a mass-forming type CC. The results of this study are consistent with those of previous reports (1 - 4,13 - 16).

In this study, ancillary findings as well as morphologic or enhancing features of the lesion were helpful in differentiating between the two diseases. The presence of an air-biliary gram is one of the factors found to be a significant predictor for hepatic abscesses. Among the four main routes for hepatic abscesses, i.e. ascending, portal, hematogenous, and iatrogenic, ascending infections were the most common cause of hepatic abscesses. From this point of view, the result of the air-biliary gram which suggests free communication between the bile duct and the enteric system was a significant CT finding for hepatic abscesses. We can also assume that reactive changes such as atelectasis of the lower lungs, pleural effusion or THAD associated with hyperemic changes could be observed more frequently in benign inflammatory lesions, and our results support this premise.

In conclusion, specific CT findings including multilayered, clustered or rim-like enhancement patterns can be helpful in diagnosing hepatic abscesses and mass-forming type CC. In addition, ANNs may potentially improve a radiologist's performance and assist in differentiating CC from hepatic abscesses, especially in the trainees with little experience in interpreting CT images.

References

1. Mathieu D, Vasile N, Fagniez PL, Segui S, Grably D, Larde D. Dynamic CT features of hepatic abscesses. *Radiology* 1985; 154:749-752
2. Jeffrey RB Jr, Tolentino CS, Chang FC, Federle MP. CT of pyogenic hepatic microabscesses: the cluster sign. *AJR Am J Roentgenol* 1988;151:487-489
3. Rubinson HA, Isikoff MB, Hill MC. Morphologic aspects of hepatic abscesses: a retrospective analysis. *AJR Am J Roentgenol* 1980; 135:735-740
4. Halvorsen RA, Korobkin M, Foster WL, Silverman PM, Thompson WM. The variable CT appearance of hepatic abscesses. *AJR Am J Roentgenol* 1984;141:941-946
5. Subramanyam BR, Balthazar EJ, Raghavendra BN, Horii SC, Hilton S, Naidich DP. Ultrasound analysis of solid-appearing abscesses. *Radiology* 1983;146:487-491
6. Gabata T, Kadoya M, Matsui O, Kobayashi T, Kawamori Y, Sanada J, et al. Dynamic CT of hepatic abscesses: significance of transient segmental enhancement. *AJR Am J Roentgenol* 2001;176:

675-679
7. Mortele KJ, Ros PR. Cystic focal liver lesions in the adult: differential CT and MR imaging features. *Radiographics* 2001;21:895-910
8. Murphy BJ, Casillas J, Ros PR, Morillo G, Albores-Saavedra J, Rolfes DB. The CT appearance of cystic masses of the liver. *Radiographics* 1989;9:307-322
9. Ryan RS, Al-Hashimi H, Lee MJ. Hepatic abscesses in elderly patients mimicking metastatic disease. *Ir J Med Sci* 2001;170:251-253
10. Jan YY, Yeh TS, Chen MF. Cholangiocarcinoma presenting as pyogenic abscess: is its outcome influenced by concomitant hepatolithiasis? *Am J Gastroenterol* 1998;93:253-255
11. Jin GY, Lee JM, Yu HC, Mun WS, Kim CS. Intraductal papillary cholangiocarcinoma with aneurismal dilation: a case of the mimicking abscess. *Hepatogastroenterology* 2002;49:1523-1525
12. Gates LK Jr, Cameron AJ, Nagorney DM, Goellner JR, Farley DR. Primary leiomyosarcoma of the liver mimicking liver abscess. *Am J Gastroenterol* 1994; 89: 1541-1543
13. Kim TK, Choi BI, Han JK, Jang HJ, Cho SG, Han MC. Peripheral cholangiocarcinoma of the liver: two-phase spiral CT findings. *Radiology* 1997;204:539-543
14. Choi BI, Han JK, Shin YM, Baek SY, Han MC. Peripheral cholangiocarcinoma: comparison of MRI with CT. *Abdom Imaging* 1995; 20:357-360
15. Choi BI, Lee JM, Han JK. Imaging of intrahepatic and hilar cholangiocarcinoma. *Abdom Imaging* 2004;29:548-557
16. Maetani Y, Itoh K, Watanabe C, Shibata T, Ametani F, Yamabe H,, et al. MR imaging of intrahepatic cholangiocarcinoma with pathologic correlation. *AJR Am J Roentgenol* 2001;176:1499-1507
17. Chan JH, Tsui EY, Luk SH, Fung AS, Yuen MK, Szeto ML, et al. Diffusion-weighted MR imaging of the liver: distinguishing hepatic abscess from cystic or necrotic tumor. *Abdom Imaging* 2001;26: 161-165
18. Henschke CI, Yankelevitz DF, Mateescu I, Brettle DW, Rainey TG, Weingard FS. Neural networks for the analysis of small pulmonary nodules. *Clin Imaging* 1997;21:390-399
19. Asada N, Doi K, MacMahon H, Montner SM, Giger ML, Abe C, et al. Potential usefulness of an artificial neural network for differential diagnosis of interstitial lung diseases: pilot study. *Radiology* 1990;177:857-860
20. Ashizawa K, Ishida T, MacMahon H, Vyborny CJ, Katsuragawa S, Doi K. Artificial neural networks in chest radiography: application to the differential diagnosis of interstitial lung disease. *Acad Radiol* 1999;6:2-9
21. Ashizawa K, MacMahon H, Ishida T, Nakamura K, Vyborny CJ, Katsuragawa S, et al. Effect of an artificial neural network on radiologists' performance in the differential diagnosis of interstitial lung disease using chest radiographs. *AJR Am J Roentgenol* 1999; 172:1311-1315
22. Wu Y, Giger ML, Doi K, Vyborny CJ, Schmidt RA, Metz CE. Artificial neural networks in mammography: application to decision making in the diagnosis of breast cancer. *Radiology* 1993;187: 81-87
23. Cross SS, Harrison RF, Kennedy RL. Introduction to neural networks. *Lancet* 1995;346:1075-1079
24. Metz CE. ROC methodology in radiologic imaging. *Invest Radiol* 1986;21:720-733
25. Metz CE. Some practical issues of experimental design and data analysis in radiological ROC studies. *Invest Radiol* 1989;24:234-245
26. Blachar A, Federle MP, Ferris JV, Lacomis JM, Waltz JS, Armfield DR, et al. Radiologists' performance in the diagnosis of liver tumors with central scars by using specific CT criteria. *Radiology* 2002;223:532-539
27. Nino-Murcia M, Olcott EW, Jeffrey RB Jr, Lamm RL, Beaulieu CF, Jain KA. Focal liver lesions: pattern-based classification scheme for enhancement at arterial phase CT. *Radiology* 2000;215:746-751
28. Kaneko T, Nakao A, Oshima K, Iizuka A. Rapid progression of intrahepatic cholangiocarcinoma after drainage of large cystic lesions: report of a case. *Surg Today* 2000;30:1049-1052
29. Chen CM, Chou YH, Han KC, Hung GS, Tiu CM, Chiou HJ, et al. Breast lesions on sonograms: computer-aided diagnosis with nearly setting-independent features and artificial neural networks. *Radiology* 2003;226:504-514
30. Nakamura K, Yoshida H, Engelmann R, MacMahon H, Katsuragawa S, Ishida T, et al. Computerized analysis of the likelihood of malignancy in solitary pulmonary nodules with use of artificial neural networks. *Radiology* 2000;214:823-830
31. Abe H, Ashizawa K, Li F, Matsuyama N, Fukushima A, Shiraishi J, et al. Artificial neural networks for differential diagnosis of interstitial lung disease: results of a simulation test with actual clinical cases. *Acad Radiol* 2004;11:29-37

대한영상의학회지 2005;53:343 - 352

종괴형 간담도암과 간농양의 감별: CT소견의 인공신경망 적용[1]

[1]서울대학병원 진단방사선과
[2]울산의대 아산병원 진단방사선과

성낙종 · 이정민 · 김세형 · 한준구 · 김영준 · 김지훈 · 이재영 · 박성호[2] · 최병인

목적: 간담도암과 간농양의 감별진단에 유용한 CT소견을 알아보고, 인공신경망이 진단방사선과 의사의 수행향상에 도움이 되는지를 알고자 하였다.
대상과 방법: 51명의 종괴형 간담도암 환자와 70명의 간농양 환자의 CT소견을 3명의 방사선과의사가 병변의 형태와 조영소견에 따라 분석하였다. 인공신경망은 이 분석으로 얻어진 유의한 소견을 이용하여 훈련되었으며 인공신경망 및 방사선과의사의 수행능력은 Receiver Operating Characteristic Analysis로 평가하였다.
결과: 테두리조영증강, 림프절종대, 피막수축, 국소담관확대, 고형성분등은 간담도암의 중요 소견이었으며 군집성모양, 다층조영증강, 뚜렷한 경계, 둥근 모양과 담도내공기등은 간농양의 중요소견이었다($p < 0.05$). 인공신경망(AZ=0.9673, 98.0%, 97.1%, and 97.5%)은 두 질환의 감별진단에 있어서 전공의(AZ=0.898, 78.4%, 81.4%, 80.2%)보다 좋은 수행능력을 보여주었다: (AZ, 민감도, 특이도, 정확성)($p < 0.05$) 그러나, 인공신경망과 전문의 사이에는 수행능력에 유의한 차이는 없었다.
결론: 몇가지 CT소견은 간담도암과 간농양의 감별에 유용하며 인공신경망은 진단방사선과 전공의들의 수행능력 향상에 도움을 준다.